EFFECT OF MICROSTRUCTURES IN LITHIUM ION BATTERY ELECTRODES

An Undergraduate Research Scholars Thesis

by

MALCOLM THOMAS STEIN IV

Submitted to Honors and Undergraduate Research
Texas A&M University
in partial fulfillment of the requirements for the designation as

UNDERGRADUATE RESEARCH SCHOLAR

Approved by
Research Advisor: Dr. Partha P. Mukherjee

May 2013

Major: Mechanical Engineering

TABLE OF CONTENTS

ABSTRACT

Effect of Electrode Microstructure on Lithium Ion Electrodes. (May 2013)

Malcolm Stein IV
Department of Mechanical Engineering
Texas A&M University

Research Advisor: Dr. Partha Mukherjee
Department of Mechanical Engineering

In a Lithium-ion battery, increases in the effective conductivity can lead to a reduction in internal cell resistance and improved cell performance. Previous efforts to improve cell conductivity have focused on the effect of conductive additives in the electrode, but particle interaction within the electrode plays a critical role. This study investigates the effect of Li-ion particle shape on the effective conductivity of Li-ion battery electrodes. Generated 3D electrode microstructure models consisting of active material, binder, conductive additive, and an electrolyte are based on macroscopic parameters or imported experimental data. This work considers spherical, cylindrical, and cubic electrode active materials for virtual material analysis. The effective conductivity was evaluated using these 3D microstructures. The effective conductivity of the electrode was found to be indirectly dependent on the shape of the active material within the electrode. This virtual electrode simulation offers a theoretical guideline for optimal Li-ion electrode battery design.

ACKNOWLEDGEMENTS

CHAPTER I

INTRODUCTION

Increasing concerns about rising fuel prices, energy security, and climate change have given rise to interest in the adoption of alternative fuels in place of traditional, petroleum-based fuels. Despite growing interest, the implementation and usage of alternative fuels has been limited by a lack of effective storage and transportation mediums. Improvements in the energy density and durability of lithium ion batteries have made them an attractive means of energy transportation and storage. Further improvements in lithium ion technology would increase the viability of alternative fuel sources and thus assist in their widespread adaptation.

In the past, implementation of batteries in vehicle design was limited to supporting roles such as ignition and lighting due to difficulties associated with the development of reversible, cost effective electrochemical systems. Today however, major car manufacturers such as General Motors, Nissan, and Toyota all have electric or hybrid vehicles on the market. This is primarily due to improvements in the overall efficiency and cost effectiveness of batteries as a means of storage and transportation of energy. Lithium ion technology is one of the battery systems used in many of the electric and hybrid vehicles on the market. Improvements in the capacity of lithium ion batteries would increase the effective range of electric vehicles and increase their safety.

Lithium ion technology can also be applied to grid energy storage. Consumer demand for electricity fluctuates based on a number of factors, including time and environmental factors. In

order to deal with these fluctuations in demand, it is more efficient to store excess power in times of low demand and use it up in times of high demand, rather than adjusting production to meet the unpredictable loads. Lithium ion batteries are an obvious choice for storage due to its excellent cyclability as compared to other battery types. If the amount of energy discharged from the battery is kept small, stresses within the electrodes can be kept a minimum, thereby extending their cyclability. Improvements in the capacity of Lithium ion batteries would allow for smaller discharges per cycle, thus extending the lifetime of the batteries.

Despite the wide range of ideal applications for Lithium ion batteries, there is still room for improvement in their performance, as previously mentioned. The performance of batteries, regardless of type, is dependent on the materials that that form the positive and negative electrode, the choice of electrolyte, and the cell architecture [5]. One of the main barriers to the improvement of Lithium ion batteries is conduction within the electrodes. The efficiency of Li-ion batteries depends, in part, on the ability of the electrodes to conduct electrons. Generally, a battery is composed of an anode, cathode, porous separator, and current collectors, as shown below in Figure 1.
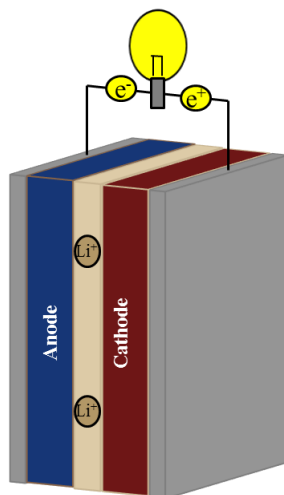
Figure 1. Typical sandwich-type lithium ion battery configuration.

A typical Li-ion electrode is composed of a combination of active material, conductive filler, binder, and void space that is filled with an electrolyte. The addition of conductive additives improves the efficiency of electrodes by reducing the internal resistance. The conductive additives are attached to the cathode by means of a binder. The incorporation of the additive and binder into a traditional 2-D architecture can be seen below. In the figure, the red spherical particles represent the active material, the green disks represent the conductive additive, the continuous blue material represents the binder, and the tan region represents the electrolyte.
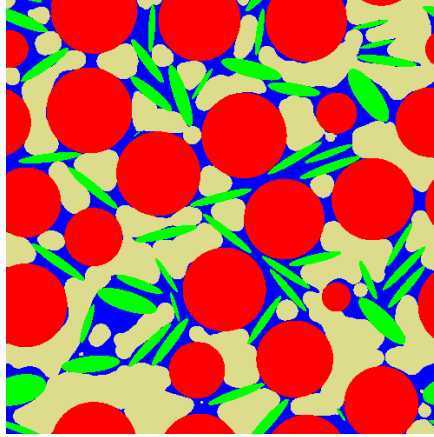
Figure 2. Conductive additive incorporation through the addition of graphite.

The inclusion of conductive additive is crucial for the efficient transport of electrons through the electrode. However, since the ability of additives to improve conductivity is dependent on the formation of conductive pathways through the material, interactions with other particles in the electrode, such as binder, active material, and the electrolyte, have a large impact on the effective conductivity of the electrode [6].

Interactions between the binder, conductive additive, and active material particles have been previously studied by Liu et. Al [7]. It was found that at a specified ratio of conductive additive to binder, the bulk conductivity of electrode laminates increased with decreasing active material content. With decreasing amounts of active material, the conductive additive and binder phase became dominant, approaching the conductivity of a pure additive and binder phase. With higher active material loadings (approximately 50% by volume) conductivities of electrodes with different additive to binder ratios are very low and similar to one another.

It is clear that the content of components within a Li-ion battery plays a role in the bulk conductivity of the electrode, but the shape of the individual particles should also be significant. Variations in the shape of conductive additives have been shown to affect the performance of Li-ion electrodes, but the shape of the active material particles has not been considered [7].

In order to determine the relationship between the active particle shape and conductivity, a stochastic modeling technique was used to create electrodes consisting of four distinct phases (active material, binder, conductive additive, and electrolyte). The active material, binder, and conductive additive content were systematically changed to observe the shape effect at varying active material contents. The effective conductivity was then evaluated using ohm's law and the conductivities of each electrode component. This understanding of the effective conductivity can be used to determine the preferred particle size and shape that results in the largest capacity and overall effectiveness.

CHAPTER II

METHODS

Stochastic modeling

The stochastic modeling technique is a method by which the geometric characteristics of a given microstructure are used to generate a representative 3D model. The generated models are then fitted by choosing parameters such that the characteristic properties of the material are realistically represented [9]. This method takes into account the macroscopic homogeneity present in the actual structures, while allowing for the random distribution of objects within the generated structures. The utilization of stochastic modeling is demonstrated in Figure 1.
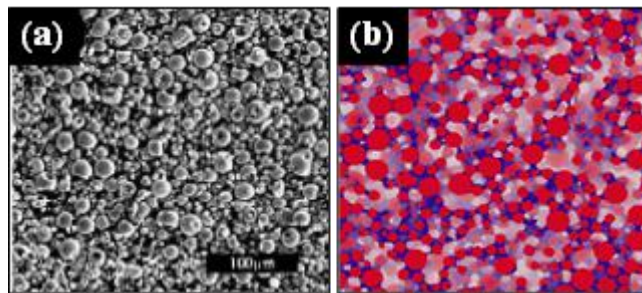

Figure 1. (a): SEM image of battery electrode. (b): Stochastic representation of (a) [10, 11].

The active material particles are generated as small spheres of varying size, and a binder is represented as continuous matter in between areas where two spheres are close.

Governing equation and boundary conditions

In order to determine the effective conductivity of multi-component porous media it is necessary to solve the stationary conduction equation in three dimensions. This can be written as

$$\nabla(\sigma \nabla V) = \dot{I} \quad \text{in } \Phi \tag{2.1}$$

where V is the potential, σ is the local electrical conductivity, $\dot{I}$ is a source term, and Φ is the domain under consideration. Several methods, such as finite difference or analytical, have been previously used; however they are lacking in terms of computational efficiency when dealing with large, complex geometries [12]. Weigmann and Zemitis solved the energy equation by harmonic averaging and introducing discontinuities or jumps in the materials as variables [13]. The interface between each object within the generated structures is continuous such that the potential is the same for the two objects on opposite sides of an interface. The Schur-complent formulation for each new variable is then solved using a combination of FFT and BiCGStab methods. This method is implemented in the simulation package GeoDict, which was used to generate the structures and determine their effective conductivities.

Modeling domain

The computational domains must necessarily represent small volumes to alleviate computational intensity, so size effect has to be taken into account. As such, a domain length to particle diameter ratio was set to 5 for the initial spherical active particle [6]. Variations in the shape of the active particle were assumed negligible. The representative volume was set to 50 μm × 50 μm × 50 μm, with a voxel size of 0.5 μm. The structures were created using voxel-based modeling. That is, the 3D structures were represented as a series of small volume elements that each represents a value on a grid in three-dimensional space.

Model parameters

A series of SEM images, shown in Figure 2, were used to determine the modeling parameters for the particles present within the electrode.
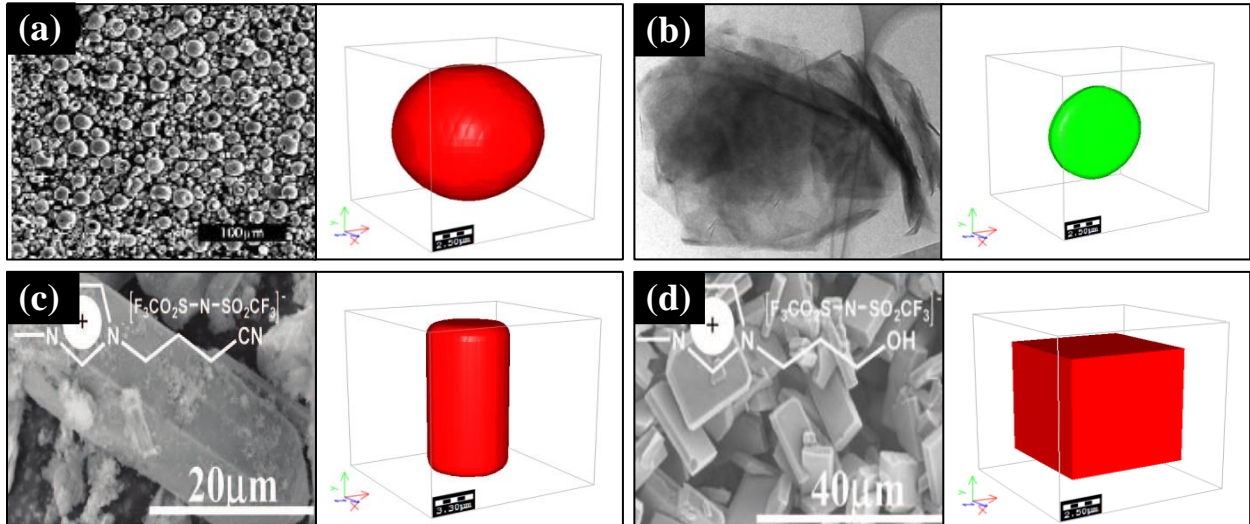

Figure 2. Stochastic modeling geometries for electrode constituents. (a): Spherical active material particles and stochastic representation [10]. (b): Graphite particle and stochastic representation [14]. (c): Cylindrical active material particle and stochastic representation [15]. (d): Cubic active material particle and stochastic representation [15].

The active material was modeled as a sphere, cube, and cylinder in each set of trials. The properties of $LiNi_{0.8}Co_{0.15}Al_{0.05}O_2$ were used to generate the initial spherical particles, with the dimensions of the remaining particles set with equal volumes. Only cathodes were considered in this study, so no other active materials were used. Graphite particles were modeled as thin spherical disks with aspect ratios a/b, a/c, and b/c set to 1, 7.4, and 7.4, respectively [6]. The dimensions of each particle can be seen below in Table I.

TABLE I. Active Particle Dimensions.

Particle	Length	Diameter	Volume	Surface Area
Sphere[6]	--	10.0 µm	5.24 E-16 m^3	31.4 E-9 m^2
Cylinder AM	13.867 µm	6.933 µm	5.24 E-16 m^3	37.75 E-9 m^2
Cube AM	8.059 µm	--	5.24 E-16 m^3	38.97 E-9 m^2

The binder was added into the generated electrodes in locations where two or more objects were close together. The remaining void space was filled with a continuous electrolyte phase. The stages of an electrode fabrication process are illustrated in Figure 3.
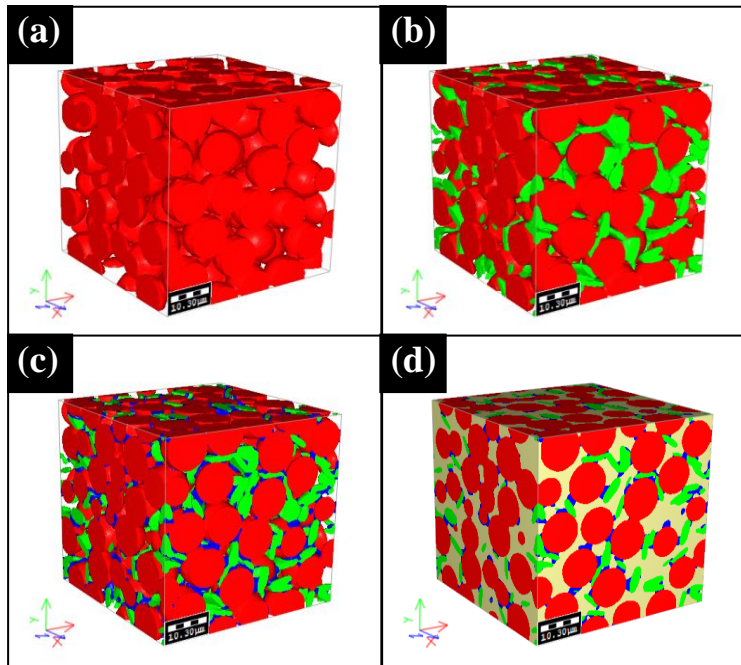

Figure 3. Electrode build process, as shown proceeding from left to right, then down. (a): Electrode is filled with active material particles (b): Conductive additives are added to the electrode (c): Binder is added between the active material and conductive additive particles (d):
Remaining space is filled with an electrolyte.

The electric conductivities of each material are listed below in Table II.

TABLE II. Component Electrical Conductivities.

Material	Electrical Conductivity
Active Material	1 S/m
Electrolyte	10 S/m
Graphite[6]	1.0×10^4 S/m
PVDF[16]	1.0×10^{-13} S/m

The original estimations for the electrical conductivities of the active material and the electrolyte are approximately one order of magnitude higher than typical values observed for those materials. However, due to the nature of the results obtained from this study and the relatively high conductivity of the conductive additive, the results are expected to be unaffected by this overestimation.

Representative elementary volume

The concept of representative elementary volume is used to identify the smallest volume over which a measurement can be made that is representative on an entire heterogeneous system. The coefficient of variation (CV) can be used as an estimate of the variability of an effective property. The CV is given as

$$CV = \frac{\sigma}{\mu} \tag{2.2}$$

where σ is the standard deviation and μ is the arithmetic mean. A CV of less than 0.5 indicates

homogeneity, with a value above 0.5 indicating heterogeneity [17].

To ensure that the generated models were free from variation of size effect, the coefficient of

variation was evaluated for the final conductivity data. The correction factor [1+1/4(N-1)] was

used when calculating the coefficient of variation due to the small sample size of 5. As shown in

Figure 4, the coefficient of variation remained under 0.16 for each electrode that was evaluated.

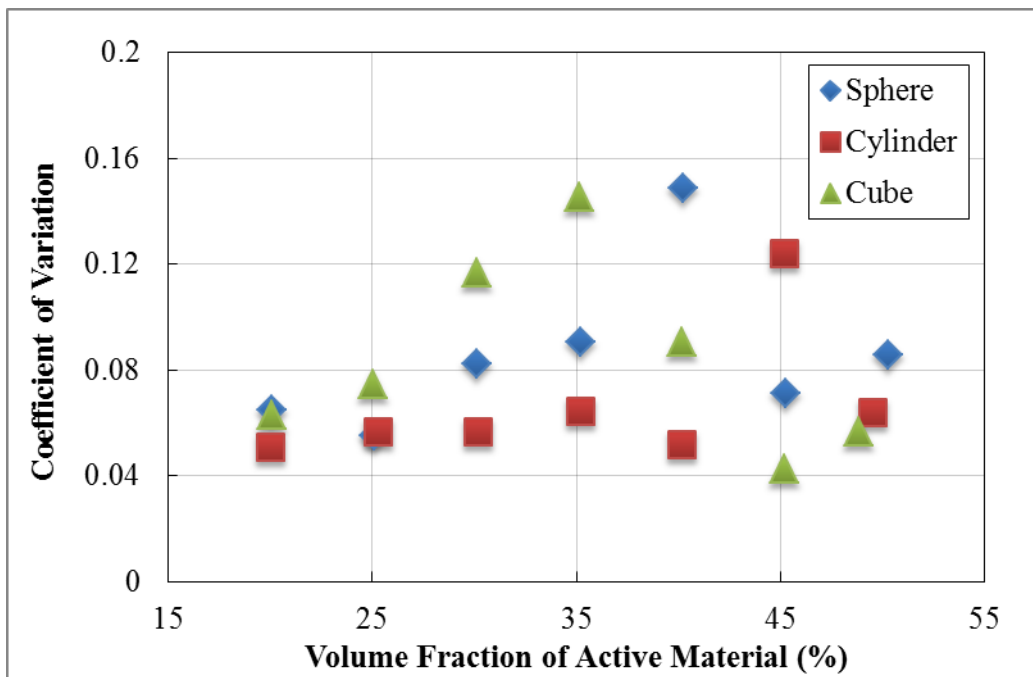**Figure 4.** Coefficient of variation for each of the evaluated electrodes.

Multiple-Phase bounds

Due to the random nature of stochastically generated models, it is often difficult to empirically

predict their properties. An alternative to empirical correlations is the usage of property bounds,

which give an upper and lower limit on the expected behavior of randomly generated structures.

These bounds incorporate microstructural information and can be applied to arbitrarily complex structures. Two types of bounds that can be applied to microstructures consisting of more than two components are Hashin-Shtrikman (H-S) bounds and Weiner bounds [18,19,20].

The H-S bounds can be applied to isotropic structures and are independent of the pore structure of the microstructure. The lower and upper H-S bounds for the electrical conductivity of an isotropic mixture of (3+1) components with thermal conductivities of σ_0, σ_1,..., σ_4, where $\sigma_0 < \sigma_1 ... < \sigma_N$, and volume fractions ϕ_0,..., $\phi_N \in [0,1]$ are given below as

$$\sigma_{H-S}^L = \sigma_0 + \frac{3\sigma_0[\phi_1/(1+f_{1-0})+\phi_2/(1+f_{2-0})+\phi_3/(1+f_{3-0})]}{\phi_0 + \phi_1 f_{1-0}/(1+f_{1-0})+\phi_2 f_{2-0}/(1+f_{2-0})+\phi_3 f_{3-0}/(1+f_{3-0})]} \qquad (2.3)$$

$$\sigma_{H-S}^U = \sigma_3 + \frac{3\sigma_3[\phi_0/(1+f_{0-3})+\phi_1/(1+f_{1-3})+\phi_2/(1+f_{2-3})]}{\phi_3 + \phi_0 f_{0-3}/(1+f_{0-3})+\phi_1 f_{1-3}/(1+f_{1-3})+\phi_2 f_{2-3}/(1+f_{2-3})]} \qquad (2.4)$$

where

$$f_{1-0} = \frac{3\sigma_0}{\sigma_1 - \sigma_0} \qquad f_{2-0} = \frac{3\sigma_0}{\sigma_2 - \sigma_0} \qquad f_{3-0} = \frac{3\sigma_0}{\sigma_3 - \sigma_0} \qquad (2.5\text{-}2.7$$

$$f_{0-3} = \frac{3\sigma_3}{\sigma_0 - \sigma_3} \qquad f_{1-3} = \frac{3\sigma_3}{\sigma_1 - \sigma_3} \qquad f_{2-3} = \frac{3\sigma_3}{\sigma_2 - \sigma_3} \qquad (2.8\text{-}2.10)$$

The Weiner bounds are applicable for both isotropic and anisotropic structures. They were derived assuming the combinations of materials as shown in Figure 5.
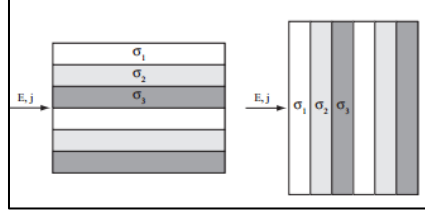
15

Figure 5. Physical material orientation used in deriving Weiner bounds. **[Adapted from 19]**

The resistances in parallel represent lowest resistance and upper limit of conductivity, whereas resistors in series represent highest possible resistance and lower limit on conductivity. The upper and lower Weiner bounds are given below as

$$\overline{\sigma}_{max} = \langle \sigma \rangle = \sum_i \phi_i \sigma_i \qquad (2.11)$$

$$\overline{\sigma}_{min} = \langle \sigma^{-1} \rangle^{-1} = \frac{1}{\sum_i \dfrac{\phi_i}{\sigma_i}} \qquad (2.12)$$

Two-Phase bounds

For the case of ion transport in a battery (or electrode), there is an electrolyte conducting phase and a solid phase that is not ionically conductive. In this type of situation, the conductivity of all phases, except electrolyte, are assumed to be zero. The percolation and Bruggeman equations give expressions for the effective conductivity of a two-phase porous electrode [19]. The percolation equation serves to quantify the conductivity of random media due to geometrical connectivity of particles. The lower limit for the percolation equation is assumed to be equal to the lowest component conductivity, while the upper limit is given as

$$\overline{\sigma}_{perc} \cong \begin{cases} \sigma_p (\dfrac{\varepsilon_p - \varepsilon_c}{1 - \varepsilon_c})^2 & \varepsilon_c \leq \varepsilon_p \leq 1 \\ 0 & 0 \leq \varepsilon_p \leq \varepsilon_c \end{cases} \qquad (2.13)$$

16

where σ_p is the pore phase conductivity, ε_p is the volume fraction of the pore phase, and ε_c is the critical volume fraction for percolation.

The Bruggeman equation is an empirically obtained formula used to relate effective conductivity with porosity. The lower bound of this formula is zero, and the upper bound is given by

$$\bar{\sigma}_B = \varepsilon_p^{3/2} \sigma_p \tag{2.14}$$

CHAPTER III

RESULTS

Stochastic Model Validation

In order to validate the premise of stochastic modeling, a separate 3D microstructure was made

to correspond with experimental results obtained by Liu et al. In their study, electrodes were

created with varying amount of active material and a changing ratio of conductive additive to

binder. In this case the active material percentages chosen were 98.8, 97.6, 96.4, 95.2, 90.4, 88.0,

82.0, 76.0, and 64% by mass. The ratio of acetylene black (AB), the conductive additive, to

polyvinylidine difluoride (PVDF), the binder, was varied between 0.2:1 to 0.8:1. The electrical

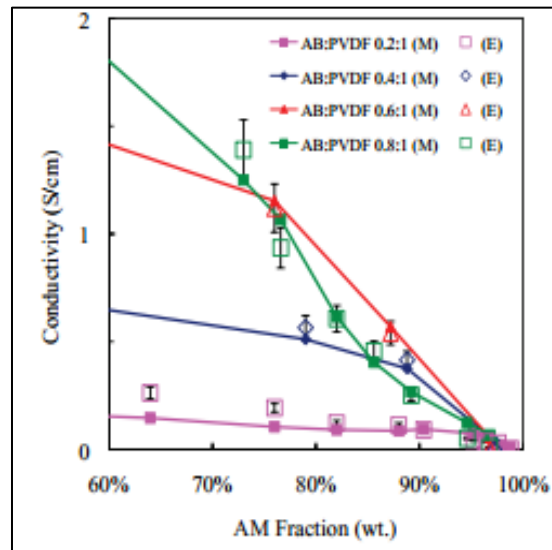conductivities of the prepared electrodes can be seen below in Figure 1.

Figure 1. Electric conductivities of electrodes at varying composition based on experimental
measurements using a four-point probe [**Adapted from 5**].

A stochastic model was created using spherical active material particles as previously mentioned, with the conductive additive modeled as short circular fibers. The electrolyte was neglected during the experimental electrode construction. As such, the 3D structures only had active material, conductive additive, and binder. The results can be seen below in Figure 2.
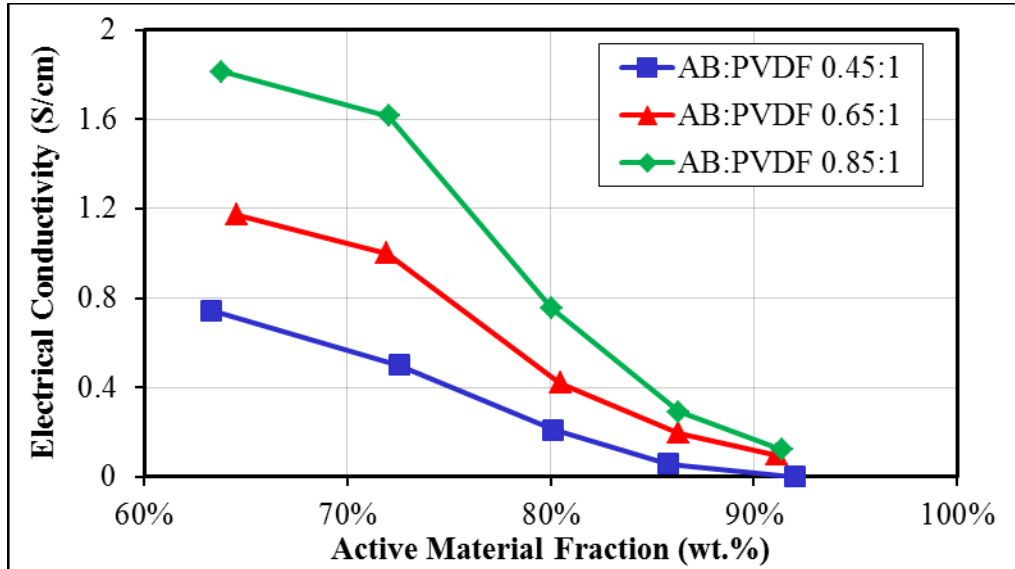

Figure 2. Effective conductivities of stochastic electrode models.

In the experimental trials, percolation was typically achieved at approximately 4 weight % AB. The stochastic model achieved percolation at roughly 4 weight % as well, indicating agreement between expected and empirical behavior. Moreover, a clear trend exists in the experimental data and the model results as it pertains to the variation in effective conductivity with varying active material percentages and AB/PVDF ratios. With decreases in the amount of active material present, the effective conductivity increases due to the increase in the AB/PVDF composite present. As the ratio of AB/PVDF increases, the effective conductivities observed in the stochastic model increase, but the effective conductivities of the experimental electrodes deviate

from this with an AB/PVDF loading of 0.8:1. Although the stochastic model does not perfectly

mimic the behavior of the experimental results obtained by Liu et al., the close similarity in the

trends in the data indicate at least moderate modeling success.

Effective conductivity

Simulation results for the effective electrical conductivities for each set of electrodes are reported

in Figure 3 below. Averaged data were plotted in the figure, with error bars of $\pm\sigma$.

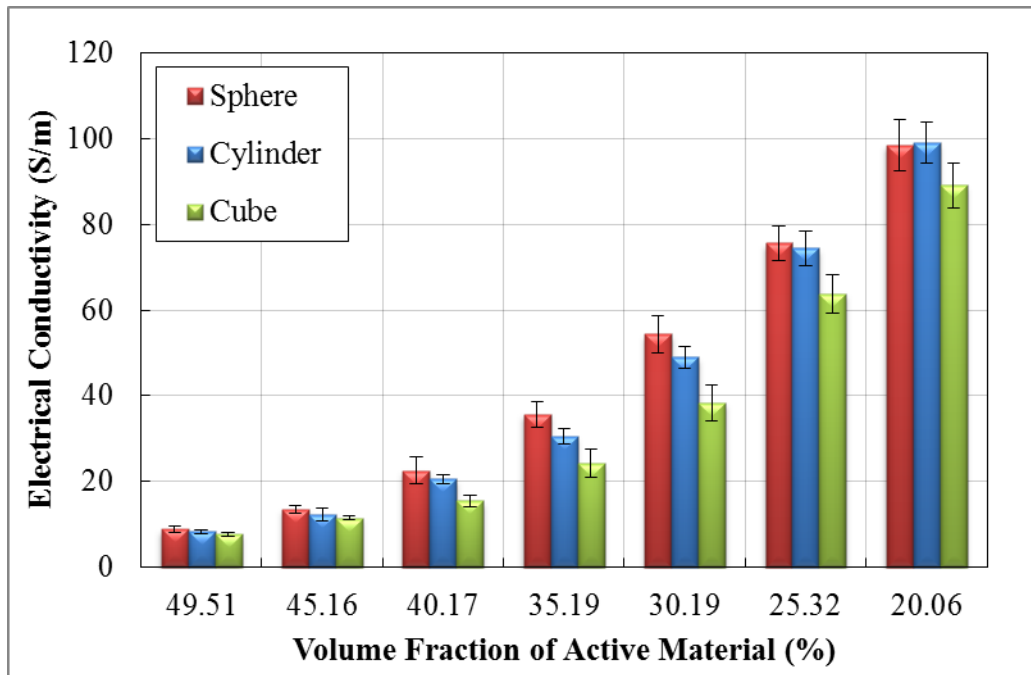**Figure 3.** Average effective conductivities for each electrode for active material loadings ranging from
49.51% to 20.06%.

For active material loadings above 40%, there is no statistically significant difference in the

evaluated electrical conductivities for all three active material shapes. At loadings below 30%,

the variation in conductivity between the cylinder and sphere is not significant. However, both

the cylinder and sphere exhibit higher electrical conductivities than the cube by approximately 9-15%, based on the averages. For the active material loading of 30%, a clear hierarchy exists in terms of average values, but there is no statistically significant difference between the sphere and cylinder. At a loading of 35%, there is a statistically significant hierarchy between the sphere, cylinder and cube. As expected, increases in the amount of conductive additive and binder result in an increase in the conductivity of the electrode, regardless of active material particle shape.

The trends in the data suggest that a more compact active particle shape will improve the conductivity of the electrode at moderate active material loadings. The formation of conductive pathways is hindered by the active material, whose particle size and shape can adversely affect pathway formation. This can be quantified in terms of the tortuosity of the electrodes before the conductive additives are added. The averaged tortuosities of each base electrode before the addition of conductive additives can be seen below in Figure 4.
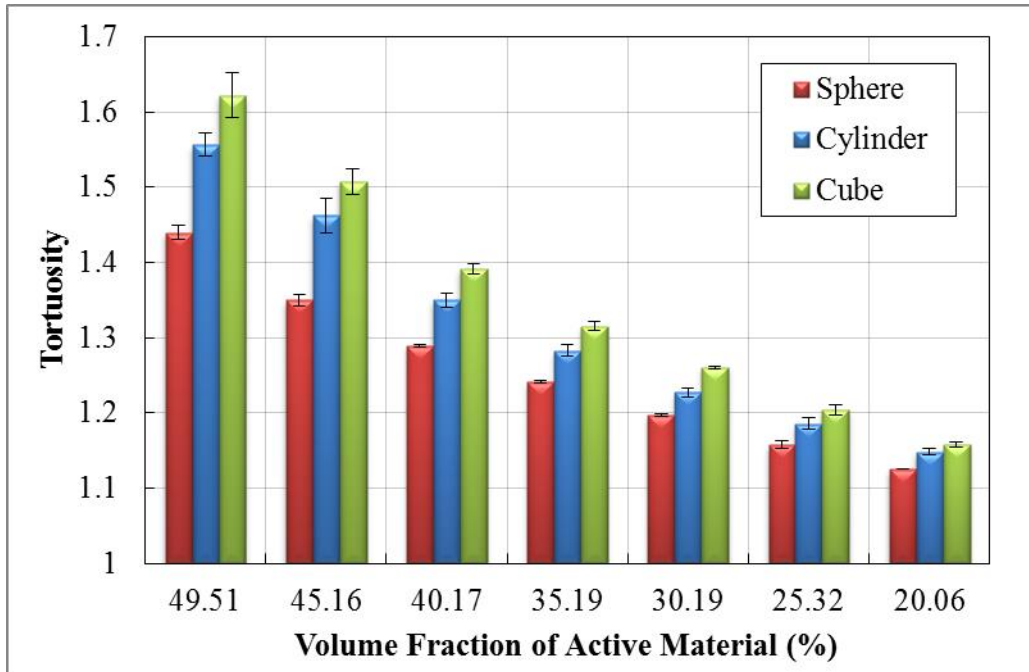
Figure 4. Averaged tortuosities in each electrode.

At every active material loading a hierarchy exists between the sphere, cylinder, and cube in terms of tortuosity. At active material loadings greater than 40%, the density of the structure restricts the ability of conductive additives to form pathways, regardless of active material shape. This indicates that above a certain tortuosity threshold, the formation of pathways is very difficult with the low amount of additives present within the structures. As the active material volume percent decreases, the tortuosity decreases for all active material particle shapes. For the loadings of 30% and 35%, increases in the tortuosities correspond to a decrease in the effective conductivities. However, at loadings of 25% and 20% the conductivities of the sphere and cylinder are roughly the same, despite their tortuosity differences. This seems to indicate a minimum tortuosity threshold below which the formation of conductive pathways is independent of active material particle shape.

A set of electrodes whose behavior matched that of the average data was used to analyze the microstructure at a closer level. The number of percolation paths and the tortuosities of the conductive system are given below in Table I.

Table I. Characteristics of conductive pathways.

	Conductive Paths	Conductivity (S/m)	Tortuosity	AM Surface Area (m^2)
Sphere				
45%	0	12.52	--	3.39e-08
35%	6	36.22	86.051	2.63e-08
30%	25	60.8	42.288	2.26e-06
25%	47	73.56	36.446	1.88e-06
Cylinder				
45%	0	12.26	--	3.88e-08
35%	3	30.30	192.67	3.11e-08
30%	9	50.90	55.266	2.66e-08
25%	28	71.74	35.96	2.25e-08
Cube				
45%	0	11.11	--	3.93e-08
35%	1	23.73	1254.93	3.13e-08
30%	6	39.72	159.672	2.69e-08
25%	34	64.69	42.4	2.23e-08

The number of conductive paths increases with decreasing active material loadings for each active material shape. As expected, this led to an increase in the effective conductivity of the electrode. However, the number of pathways alone is not an effective metric for a comparison with effective conductivity. For the active material loading of 25%, the cylinder and sphere cases have roughly the same effective conductivity, despite the large difference in conductive pathways. Similarly, the cube at 25% has a lower conductivity then the cylinder, despite the larger number of pathways. Although the cube active material loading has a higher number of pathways than the cylinder, the tortuosity of the paths is higher than that of the cylinder. This concept can also be applied to the cylinder and sphere comparison. These trends indicate that both the quantity and quality of the conductive pathways have an impact on the effective conductivity of the electrode.

Effective conductivity bounds

The multiple phase Hashin-Shtrikman and Weiner bounds and two-phase Bruggeman and percolation equations were applied using the volume percentage of each material present and their respective conductivities. The averaged data for the spherical case was plotted as well, for comparison. This can be seen in Figure 5 below.
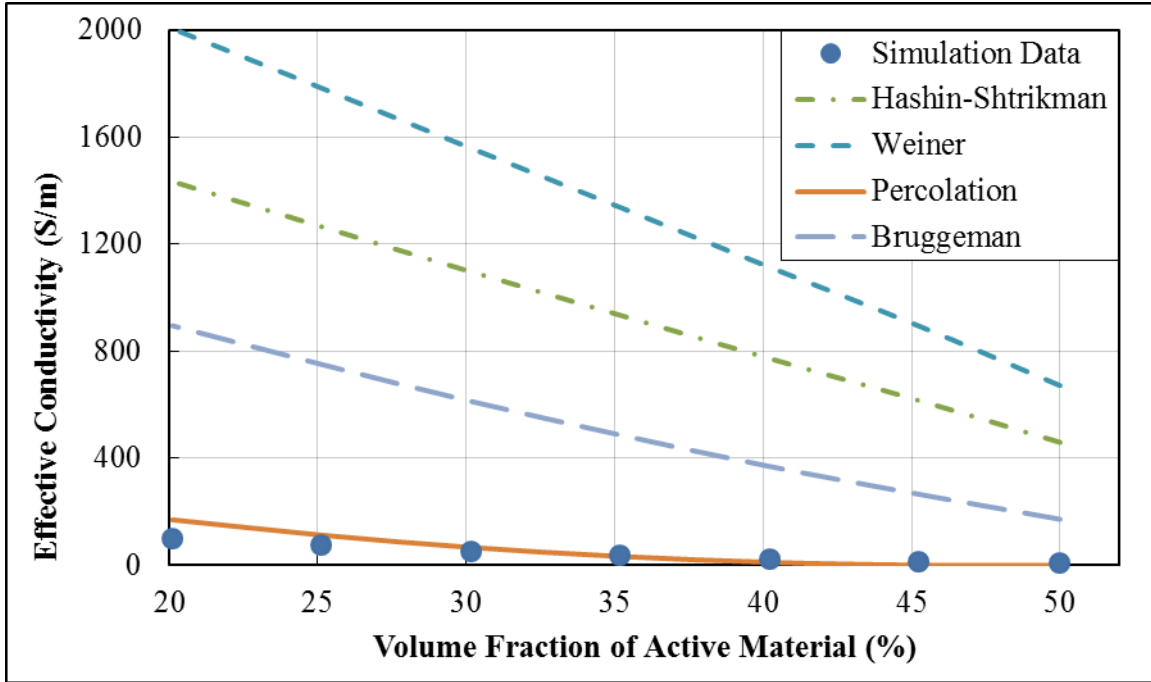
Figure 5. Effective conductivity bounds applied to averaged sphere-based microstructure data.

As can be seen above, both of the multiple-phase bounds vastly overestimate the effective

electrical conductivities of the electrodes. This is likely due to the fact that these bounds are not

meant for direct implementation with models whose properties are primarily dependent on

pathway formation of a single phase. The Bruggeman equation more closely estimates the

behavior of the electrodes, but still over predicts the conductivities by almost one order of

magnitude. Because the Bruggeman equation is meant to relate the porosity of an electrode with

its conductivity, it is better suited for the determination of ionic conductivity in liquid-electrolyte

soaked porous media than the electrical conductivity based on particle connectivity [20]. The

percolation equation is the most accurate predictor of the electrode behavior. For active material

loading less than approximately 30%, the percolation equation slightly under predicts the

effective conductivities. For loadings greater than approximately 30%, the percolation equation

over predicts the behavior of the electrodes. The close agreement between the conductivities of

the electrode models and the percolation equation is due to the fact that the percolation equation is meant to characterize the conductivity based on the random connectivity of particles within a microstructure. The central point to this is the existence of a critical volume percentage, above which conductive networks will form, and below which none will form. By utilizing the critical volume percentage from the generated structures, a more accurate representation of their behavior was obtained with the percolation equation.

CHAPTER IV

CONCLUSIONS

In this study, a stochastic modeling technique was used to model electrode microstructures of varying active material shape and loading percentage. The modeling domain was selected such that variations due to size effect were negligible. The effective conductivity was evaluated for all of the generated electrodes, and significant conclusions were drawn from the results.

The data suggested that a lower surface area to volume ratio of active particles increases the amount of continuous space available for pathway formation within the electrodes at moderate active material loadings. At higher active material loadings, the density of the structure and low additive content prevent the formation of conductive pathways through the electrode. At lower active material loadings, the formation of pathways seems to be less predictable based on the parameters utilized in this study.

The percolation equation best predicts the effective conductivity of the electrode, indicating the conductive additive dominates the conductivity of the electrode. This means that the electrode it may be treated as consisting of two phases for effective conductivity prediction based on microstructural content.

REFERENCES

1.   P.P. Mukherjee, S. Pannala, and J.A. Turner, Modeling and Simulation of Battery Systems, in Handbook of Battery Materials. 2011, Wiley-VCH Verlag GmbH & Co. KGaA: Weinheim, Germany.

2.   E.J Cairns. and P. Albertus, Batteries for Electric and Hybrid-Electric Vehicles. Annual Review of Chemical and Biomolecular Engineering, 2010. 1(1): p. 299-320.

3.   Martin, M., Modeling of Transport in Lithium Ion Battery Electrodes, in Mechanical Engineering To be published, Texas A&M University.

4.   M. Martin, P.P.Mukherjee, D. Ranjan, S. Pannala, J. Turner, J. Dietiker, Concentration Behavior in 3D Electrodes for Lithium Ion Batteries. Journal of The Electrochemical Society, To be Published.

5.   M. Armand and J.M. Tarascon, Issues and Challenges facing Rechargable Lithium Batteries. Nature, 2001. 414: p. 359-367.

6.   Y.-H. Chen, C.-W Wang, G. Liu, X.-Y. Song, V. S. Battaglia, A. M. Sastry, Selection of Conductive Additives in Li-Ion Battery Cathodes: A Numerical Study. Journal of The Electrochemical Society, 2007. 154: p. A978-A986.

7.   V. S. Battaglia, G. Liu, X. Song, and H. Zheng, Particles and Polymer Binder Interaction: A Controlling Factor in Lithium-Ion Electride Performance. Journal of The Electrochemical Society, 159(3), A214-A221 (2012).

8.   M. Chung, G. B. Less, M. Park, A.M. Sastry, and X. Zhang, A Review of Conduction Phenomenon in Li-ion Batteries. Journal of Power Sources, (2010), doi:10.1016/j.jpowsour.2010.06.060.

9.   J. Becker, P. Mukherjee, V. Schulz, C. Wang and A. Wiegmann, Modeling of Two-Phase Behavior in Gas Diffusion Medium of PEFCs via Full Morphology Approach. Journal of The Electrochemical Society, **154**, B419(2007).

10.   J. Liu et al., Long-term Cyclability of $LiFePO_4$/Carbon Composite Cathode Material for Lithium-ion Battery Application. Electrochimica Acta, 54, 5656 (2009).

11.   K. C. Smith, P. P. Mukherjee, and T. S. Fisher, Columnar Order in Jammed $LiFePO_4$ Cathodes: Ion Transport Catastrophe and its Mitigation. Physical Chemistry Chemical Physics, DOI: 10.1039/c2cp40135e (2012).

12.	G. Tsotridis and D. Veyret, Numerical Determination of the Effective Thermal Conductivity of Fibrous Materials. Application to Proton Exchange Membrane Fuel Cell Gas Diffusion Layers. Journal of Power Sources,195, 1302-1307 (2010).

13.	A. Wiegmann and A. Zemitis, EJ-Heat: A Fast Explicit Jump Harmonic Averaging Solver for the Effective Heat Conductivity of Composite Materials. Technical Report, Fraunhofer ITWM, 94(2006).

14.	François Béguin and Elżbieta Frąckowiak. Carbons for Electrochemical Energy Storage and Conversion Systems. Boca Raton: CRC, 2010. 271. CRCnetBASE. Web. 31 July 2012.

15.	M. Armand, J.M. Tarascon, et al., Ionothermal Synthesis of Tailor-Made $LiFePO_4$ Powders for Li-Ion Battery Applications. Chemistry of Materials, 21, 1096–1107 (2009).

16.	"PVDF." *Material Properties of Engineering Polymers*. N.p., n.d. Web. 25 July 2012. <http://www.matbase.com/material/polymers/engineering/pvdf/properties>.

17.	J. Becker, X. Li, J. Shen, A. Wiegmann, and N. Zamel, Estimating Effective Thermal Conductivity in Carbon Paper Diffusion Media. Chem. Eng. Sci., 65, 3994-4006 (2010).

18.	L. Jing, F. Tong, and R. W. Zimmerman, An Effective Thermal Conductivity Model of Geological Porous Media for Coupled Thermo-Hydro-Mechanical Systems with Multiphase Flow. International Journal of Rock Mechanics and Mining Sciences, 46, 1358-1369 (2009).

19.	Liu LP. Hashin-Shtrikman Bounds for Multiphase Composites and their Attainability. The Royal Society, doi:10.1098/rspa.2009.0554 (2010).

20.	M.Z. Bazant and T.R. Ferguson, Nonequilibrium Thermodynamics of Porous Electrodes. Journal of the Electrochemical Society, 159(12), A1967-A1985 (2012).

21.	C.H. Arns, E.J. Garboczi, M.A. Knackstedt, and W.V. Pinczewski, Computation of Linear Elastic Properties from Microtomographic Images: Methodology and Agreement Between Theory and Experiment. Journal of Geophysics, 67(5), 1396-1405 (2002).

22.	J. Becker, E. Glatt, L. Cheng, S. Rief, and A. Wiegmann, GeoDict 2012: Basic Volume. Fraunhofer ITWM, Version 5.4 (2012).

23.	J. Becker and A. Wiegmann, GeoDict 2012: User Module and Macros Tutorial. Fraunhofer ITWM, Version 1.0 (2012).

24.	J. Becker, E. Glatt, K. Schmidt, and A. Wiegmann, GeoDict 2012: SinterGeo Tutorial. Fraunhofer ITWM, Version 1.0 (2012).

25.   J. Becker, E. Glatt, and A. Wiegmann, GeoDict 2012: ProcessGeo Tutorial. Fraunhofer ITWM, Version 1.0 (2012).

26.   J. Becker and A. Wiegmann, GeoDict 2012: ConductoDict Tutorial. Fraunhofer ITWM, Version 1.0 (2012).

27. J. Becker and A. Wiegmann, GeoDict 2012: DiffuDict Tutorial. Fraunhofer ITWM, Version 1.0 (2012).

28.   *Predicting Long Range Interactions in Lithium Ion Electrodes*: Malcolm Stein IV, Seongkoo Cho, and Partha Mukherjee, In preparation for submission in J. Electrochem. Soc.